Wind regimes associated with a mountain gap at the northeastern Adriatic coast

Danijel Belušić*, Mario Hrastinski, Željko Večenaj, Branko Grisogono

Danijel Belušić
Monash Weather and Climate
School of Mathematical Sciences
Monash University
Melbourne, Victoria, Australia

Mario Hrastinski
Croatian Meteorological and Hydrological Service
Zagreb, Croatia

Željko Večenaj and Branko Grisogono
Department of Geophysics
Faculty of Science
University of Zagreb
Zagreb, Croatia

*Corresponding author
Danijel Belušić
School of Mathematical Sciences
Building 28
Monash University
Clayton, Victoria 3800
Australia
E-mail: danijel.belusic@monash.edu

ABSTRACT

Winds through the Vratnik Pass, a mountain gap in the Dinaric Alps, Croatia, are polarized along the gap axis that extends in the northeast-southwest direction. Although stronger northeasterly wind at the Vratnik Pass is frequently related to the Adriatic bora wind, especially at the downstream town of Senj, there are many cases when wind at Senj is directionally decoupled from wind at the Vratnik Pass. A cluster analysis reveals that this decoupling is sometimes related to lower wind speeds or shallow southeasterly sirocco wind along the Adriatic, but in many cases the bora blows over a wider region, while only Senj has different wind direction. Several mechanisms can be responsible for the latter phenomenon, including the formation of a lee wave rotor. A numerical model simulation corroborates the decoupling caused by a rotor for a single case.

The prevalence of northeasterly winds at the Vratnik Pass during southeasterly sirocco episodes is another result that challenges the current understanding. It is shown that at least in one of the episodes, this phenomenon is related to a secondary mesoscale low-pressure center in the eastern lee of the Apennines that forms as a subsystem of a broader Genoa cyclone.

Less frequent southwesterly winds through the gap are predominantly related to the thermal sea-breeze and anabatic circulations that are sometimes superimposed on the geostrophic wind.

1. Introduction

Mean wind patterns over the Adriatic were described decades ago (e.g. Makjanić 1978), and classified into four main categories: northeasterly bora, southeasterly Adriatic sirocco (jugo), northwesterly etesian and local thermal circulations (e.g. Prtenjak and Grisogono 2007; Pasarić et al. 2009). Pandžić and Likso (2005) used principal component analysis to classify wind observations along the entire eastern Adriatic coast. Their analysis resulted in 11 wind types that could be condensed into the same four categories as above with an additional near-calm wind type. Local complexities of these flow patterns have been addressed only recently, with the advance and accessibility of limited-area numerical models (e.g. Pasarić et al. 2007; Grisogono and Belušić 2009; Klaić et al. 2009a; Prtenjak and Belušić 2009; Prtenjak et al. 2010). Even more complex situations, with weak to moderate synoptic pressure gradients that are modified by local thermal circulations at the northern Adriatic coast, have been recently analysed using measurements (e.g. Orlić et al. 1988; Prtenjak 2003; Prtenjak and Grisogono 2007) and numerical modeling (e.g. Nitis et al. 2005; Prtenjak et al. 2006; 2008). A multitude of spatial flow patterns is possible under those conditions due to variable wind direction and highly complex terrain.

The dominant wind at the northeastern Adriatic is bora – for example, bora blows 177 days annually in the town of Senj (e.g. Yoshino 1976; Makjanić 1978; see Fig. 1 for the location). Bora is most frequent in the cold part of the year when persistent anticyclones over the northeastern Europe or cyclones over the Adriatic and Mediterranean ensure the supply of cold continental northeasterly air. Bora is a downslope windstorm whose basic characteristics follow the hydraulic flow dynamics with supercritical regions in the mountain lee that are dissipated in hydraulic jumps further downstream (Smith 1987). The upper flow dividing streamline descends in the lee as a result of the presence of an inversion just above the mountain top height or due to mountain wave breaking in the lee (Klemp and Durran 1987). These mesoscale mechanisms generate large cross-mountain pressure gradient and cause acceleration of wind such that the mean speeds in the lee reach 30 m s^{-1} with gusts surpassing 60 m s^{-1} (e.g. Jiang and Doyle 2005; Belušić and Klaić 2006; Gohm et al. 2008). The bora jets can extend over the entire width of the Adriatic Sea and reach its western coast (e.g. Dorman et al. 2006; Signell et al. 2010). Bora influences the coastal areas, sea state and circulation, sea and land traffic, tourism and agriculture. It is associated with several specific dynamical features, such as wave-induced rotors, quasi-periodic pulsations of gusts, and potential vorticity banners. It has therefore attracted considerable interest over the years, which has resulted in a large number of studies (see the recent review by Grisogono and Belušić (2009) and references therein).

The terrain complexity is evident along the Dinaric Alps, the mountain range that extends along the eastern Adriatic coast separating it from the interior continental region (Fig. 1). The Dinaric Alps have several gaps that influence the spatial flow patterns, particularly during the bora wind (e.g. Grubišić 2004; Belušić and Klaić 2006; Dorman et al. 2006; Gohm et al. 2008; Grisogono and Belušić 2009; Signell et al. 2010). Despite their importance, little work has been done on the examination of flow patterns through these mountain gaps, especially over an extended period of time. This study presents the first wind measurements at the Vratnik Pass (Fig. 1) that were collected over a period of about nine months. The dataset length allows for classification of wind regimes at the Vratnik Pass and the nearby coastal and island stations, which is performed using a cluster analysis. Additionally, a preliminary data analysis has indicated several unexpected flow characteristics, such as directional decoupling between the Vratnik Pass and Senj during bora (Večenaj et al. 2011). These situations are captured well by the current classification technique, which enables a more general perspective on the synoptic and mesoscale conditions that generate such situations.

The paper is organized as follows: Section 2 presents the data and main results from basic data analysis, which reveals and quantifies some of the intricacies of the local flow characteristics; Section 3 describes the cluster analysis technique; Section 4 presents and discusses the results of clustering, relates them to dominant synoptic conditions and undertakes numerical modeling to resolve the flow complexities that seem unexpected without proper data; and Section 5 concludes the study, leaving several open questions for further research.

2. Data and basic analysis

The first wind measurements at the Vratnik Pass over an extended time period, October 2004 – June 2005, provide a unique opportunity for analysis of wind regimes through a mountain gap. The Vratnik Pass is a pronounced mountain gap located in the northern part of the Dinaric Alps (Fig. 1). It is well known for its relation to the bora wind, since it is located upstream of the town of Senj that is famous for its very frequent and persistent bora cases (Poje 1992). The three wind components were recorded at 9.5 m above ground using a Gill WindMaster sonic anemometer with 4-Hz sampling frequency (Belušić and Klaić 2006). Simultaneously, the same type of instrument was located in Senj at 13 m above ground (Klaić et al. 2009b), which enables the analysis of the relationship between the winds at the Vratnik Pass and Senj. The Senj sonic anemometer was mounted on a 3-m mast on the roof of the 10-m tall Senj sea-port captaincy building. It was installed in a location different to the standard Senj weather station, because the standard station is sheltered from the bora wind directions (Klaić et al. 2009b). There were several gaps in the measurements at the Vratnik Pass, mostly shorter in duration except for the one that lasted from late March to early May 2005. Since the measurements were not gathered in the period from July to September, the situations with etesian winds, which appear during the warm part of the year, will not be taken into account in the present analysis.

We use two additional stations in the local area to provide supplementary information about the flow patterns. These two stations are taken as far away from the coast as possible on an approximately northeast–southwest line connecting them with the Vratnik Pass and Senj (Fig. 1). The reason for the latter will become obvious below, while the distance from the coast is needed to relate the flow patterns at the Vratnik Pass and Senj to the overall larger-scale wind patterns over the northeastern Adriatic. Mali Lošinj is obviously most suited for that geographically, but the limitation is that the anemometers in Mali Lošinj and

Rab are sheltered at the east and between northeast and south, respectively (Croatian Meteorological and Hydrological Service, personal communication).

In the following, the terms 'bora' and 'northeasterly wind' will sometimes be used interchangeably for convenience, disregarding the fact that northeasterly wind is a broader category because some of the northeasterly winds are of thermal origin, unlike the currently accepted dynamical origin of bora (see Grisogono and Belušić 2009). The wind roses for the two main stations, the Vratnik Pass and Senj, are depicted in Fig. 2. Winds at the Vratnik Pass are markedly bimodal and can be classified into northeasterly bora with directions from 30 – 90°, and southwesterly winds with directions ranging from 210 – 270°. This polarization is a natural consequence of the geographical orientation of the pass. However, the relationship of these two wind regimes at the Vratnik Pass to the known wind patterns at the coast is not known, and this is examined in the remainder of the paper.

The wind rose at Senj shows the known predominance of the bora wind for higher wind speeds. However, weak winds are dominantly from the southeast, which indicates that Senj and the Vratnik Pass are directionally decoupled for low wind speeds. Conditional wind roses at Senj shown in Fig. 3 provide additional insight into the level of decoupling. For weak winds at the Vratnik Pass, Senj and the Vratnik Pass are decoupled regardless of the wind direction. Similarly, for southwesterly winds at the Vratnik Pass, Senj and the Vratnik Pass are predominantly decoupled regardless of the wind speed. It is therefore obvious that the coupling between Senj and the Vratnik Pass is associated predominantly with strong northeasterly winds, and Fig. 3 shows that the stronger the bora at the Vratnik Pass, the stronger the coupling between Senj and the Vratnik Pass. The coupling starts when wind speed at the Vratnik Pass surpasses 5 m s^{-1}.

It has been almost tacitly assumed in previous studies that northeasterly winds at Senj and the Vratnik Pass are always coupled, particularly because the bora in Senj is such a predominant wind and is clearly related to the air arriving from the Vratnik Pass. The unexpected result here is that there are situations with weak, moderate and sometimes even strong bora at the Vratnik Pass when Senj does not experience bora at all (Fig. 3b, c). We will refer to these situations as decoupled bora cases.

Figure 4 depicts different possibilities of the bora occurrence simultaneously at the Vratnik Pass and Senj. The bora occurrence is based on wind direction only, and is defined for both stations as wind blowing continuously during at least 3 h from directions between 30° and 90°. This enforces a rather strict condition on the bora occurrence, but on the other hand does not allow random wind direction variability to be counted as a bora occurrence. Table 1 explains the detector values used in Fig. 4. The detector value of two, indicating the bora occurrence at the Vratnik Pass but not at Senj, i.e. the decoupled situations, appears throughout the observational period. It should be noted that this definition of a bora occurrence means that a decoupled episode can occur even when wind at Senj is between 30° and 90° but lasts less than 3 h. A number of cases with weak-to-moderate wind will naturally enter the latter category, but will not be given special consideration here. Understanding the structure and mechanisms of the other decoupled situations is the primary motivation for further analysis.

3. Clustering method

In order to gain better understanding of the local spatial wind patterns, the winds at the four chosen stations are classified using the K-means clustering method (e.g. Anderberg 1973). This method has been used in many different meteorological contexts, such as for clustering of mesoscale convective systems (e.g. Pope et al. 2009), hurricane tracks (e.g. Elsner 2003) and mesoscale wind fields (e.g. Kaufmann and Weber 1996).

We use the standard Matlab K-means algorithm with squared Euclidian distance between vectors at each observation location as the measure of similarity. Some authors have suggested using wind vectors scaled by time or space averaged winds, in order to reduce the overweighting of stations with higher wind speeds or to remove the effects of overall scaling factors for otherwise similar spatial wind patterns, respectively (e.g. Weber and Kaufmann 1995; Kaufmann and Whiteman 1999; Burlando et al. 2008; Jiménez et al. 2009). We do neither for a number of reasons. First of all, the Vratnik Pass is characterized by higher wind speeds compared to the other stations. Since we are primarily interested in detailed wind regimes through the Vratnik Pass and only secondary about other stations, this natural overweighting of the Vratink Pass assists the analysis.

Second, it will be shown later that in our case the differences between clusters that result only from overall scaling factors may point to different physical origins of similar wind patterns. Third, we use only four stations that are located in the region with already known larger-scale wind patterns (Prtenjak 2003; Pandžić and Likso 2005). This makes our analysis and decision-making simpler.

The latter also means that it is straightforward to visually determine the optimal number of clusters. The cluster analysis was performed with number of clusters increasing from two to ten and the resulting clusters were examined visually for substantial differences. Eight clusters still brought important new information compared to seven clusters, while increasing the number of clusters beyond eight resulted only in splitting of certain clusters to two almost identical wind regimes. Hence we chose eight as the optimal number of clusters in our analysis.

The reliability of the method is tested by re-running the algorithm several times. Initial cluster centroids are randomly chosen and they always converge to the same final clusters when the number of clusters is eight, which additionally supports this choice for the number of clusters (e.g. Pope et al. 2009). Further evidence of the robustness of clustering results is given in the next section.

4. Results

a. Cluster analysis

The eight cluster centroids are shown in Fig. 5. They are consistent with the results from a larger-scale classification (Pandžić and Likso 2005). There are only two clusters with southwesterly flow at the Vratnik Pass (clusters 1 and 6), while all the others are dominated by the northeasterly flow. The two clusters with southwesterly wind account for about 29% of the total number of cases. This agrees with the wind rose at the Vratnik Pass, which shows about 30% of cases with southwesterly winds (Fig. 2).

Further analysis reveals that the most distant members of individual clusters are mostly very similar to their cluster centroids both in magnitude and direction of the wind vector at all stations. Larger differences of the most distant members may occur in wind direction only for clusters and stations with weak winds, such as clusters 1 and 3, and the station Senj in cluster 7. This implies that the clusters are consistent and can be used for mapping the characteristic wind patterns.

It is possible that some of the clusters represent only transitional features with short duration. Several different tests of duration and consistence of episodes were performed and they agree that all clusters are predominantly composed of well-defined episodes. Average durations of uninterrupted episodes within each cluster are given in Table 2. Clusters 1, 2, 5 and 6 are characterized by on average longer episodes than the other four clusters. This is somewhat unexpected for clusters 2 and 5, because they are predominantly separated by small to moderate differences only in the overall wind speed, i.e. the scaling factor, and not in the direction. One would, therefore, expect numerous transitions between clusters 2 and 5 during a single bora episode – yet, continuous episodes longer that 24 h are not rare for each of the two clusters.

Likewise, the time series of cluster categories shows that successive point-to-point transitions are the most frequent between the same cluster categories and account for about 90% of transitions for clusters 1, 2, 5 and 6, and about 80% of transitions for the other four clusters. The most frequent remaining transitions between different clusters are shown in Table 2 for each cluster category. The latter illustrates typical time evolutions of different flow configurations. For example, the transitions confirm that the strongest bora, cluster 5, is simply a stronger-wind version of cluster 2, as almost all transitions to and from cluster 5 occur exclusively through cluster 2. Similarly, for southwesterly winds at the Vratnik Pass, the stronger-wind cluster 6 is reached and left predominantly through the weaker-wind southwesterly cluster 1. An even broader picture is revealed when all clusters with northeasterly winds at the Vratnik Pass and Senj are considered: clusters 3, 4, 2 and 5 form a progression of increasing northeasterly winds at both stations. Their interrelationships are also evident from the transitions: the weakest bora in cluster 3 can transition to either somewhat stronger bora in cluster 4, or, as expected for weak-wind cases, change direction and transition to the weakest southwesterly cluster 1. The moderate bora cluster 4 can go both ways, increasing (cluster 2) or decreasing wind speed (cluster 3), but not changing the wind direction at the Vratnik Pass and Senj. It can also move to cluster 7, which has strong northeasterly winds at the Vratnik Pass and moderate northeasterly winds at the two outer stations, but very weak winds at Senj when compared with the other four northeasterly clusters. This is a somewhat different flow setup and will be discussed separately. Finally, cluster 2 has two-way transitions with the weaker cluster 4 and, as mentioned before, the strongest cluster 5.

Cluster 8 represents the airflow pattern associated with the Adriatic sirocco wind (e.g. Jurčec et al. 1996; Brzović and Strelec Mahović 1999). The Adriatic sirocco frequently develops when a cyclone is located northwest of the Adriatic Sea and, assisted by the Dinaric Alps, forces the air to move along the Adriatic Sea from the southeast. As the cyclone propagates towards the southeast, the sirocco over the northern Adriatic gradually transforms to the northeasterly bora wind (e.g. Horvath et al. 2008; Pasarić et al. 2009). This is evident from the cluster transitions, where cluster 8 frequently moves to the weakest bora cluster 3, which can later result in strong bora through the aforementioned progression. It also transitions to the weakest southwesterly cluster 1, probably denoting the cessation of main synoptic forcing over the domain of interest. On the other hand, Table 2 indicates that neither of the other clusters frequently transition to cluster 8, but this is due to its rare occurrence of only 3.5% of all cases. It can be shown that the transitions for cluster 8 are two-way, so the relative majority of transitions to cluster 8 come from clusters 1 and 3.

While different bora scenarios at the Northern Adriatic coast are relatively well known from a multitude of previous studies (e.g. Grubišić 2004; Gohm and Mayr 2005; Belušić and Klaić 2006; Večenaj et al. 2010; 2012), the situations with sirocco or weak winds have received much less attention. Vukičević et al. (2005) present an analysis of the Adriatic sirocco flow on 26 December 2004 and show that the sirocco is a rather shallow phenomenon with low-level mountain-influenced southeasterly winds turning towards the synoptic southwesterly to westerly flow at heights above 1 km. This agrees with Ivančan-Picek et al. (2006), who extend the analysis to a few other sirocco cases and explain that the predominant sirocco synoptic flow is from the southwest as a result of deep cyclones approaching from the Atlantic to the western Mediterranean. While bora onset is abrupt, sirocco begins and strengthens gradually. On the mesoscale, firstly due to the Dinaric Alps stretching southeast – northwest, the mean wind turns from southwesterly aloft to southeasterly in the boundary layer. Secondly, easterly ageostrophic wind component toward the low pressure approaching from the west develops by the usual wind turning in the boundary layer. Due to these and some other characteristics of sirocco in the Adriatic, Ivančan-Picek et al. (2006) insist that this wind should have a local name "jugo". They also find that it usually does not extend over 2 km in depth; hence, this southeasterly flow often cannot make it over the coastal mountains. The sirocco pattern of cluster 8 therefore seems to contradict the expectations based on the current knowledge. While the southeasterly winds at the outer two stations are the obvious sign of sirocco, and the easterly wind at Senj could be explained by the topographic shadowing effects of the station used in this study, the clearly northeasterly wind at the elevated Vratnik Pass is puzzling because it seems to oppose the associated southwesterly geostrophic wind. In order to examine this seeming contradiction, we study the situation from 26 – 28 December 2004 in more detail in a later subsection using a numerical model.

Of particular interest here is the previously raised issue about the directional decoupling between the Vratnik Pass and Senj for northeasterly winds at the Vratnik Pass. Figure 6 shows that these cases are predominantly related to low-to-moderate wind speed clusters (3 and 4), to the sirocco cluster 8, or to the rather special bora cluster 7. Weak winds are characterized by large directional variability (e.g. Belušić and Güttler 2010; Mahrt 2011) and weak vertical coupling (e.g. Mahrt 2010). For clusters 3 and 4, this naturally results in sporadic occurrences of directional decoupling between the Vratnik Pass and Senj, and also in sporadic couplings that last less than 3 h and are not considered to be coupled cases (see Section 2). The occurrence of northeasterly wind at the Vratnik Pass is rather unexpected for the sirocco episodes in cluster 8 and, as already mentioned, this will be further analyzed later. However, even at this point it is easy to understand that with predominantly southeasterly winds over the Adriatic and northeasterly winds at the Vratnik Pass, the direction at Senj can shift between the two directions following probably only small changes of the overall flow pattern. As for cluster 7, a very interesting result is that the decoupled bora cases account for about 87% of its cases (Fig. 6). This makes cluster 7 a representative of these situations. The cluster 7 centroid has northeasterly wind at all stations, but the difference to the usual bora cases is that the wind magnitude at Senj is considerably smaller than at the Vratnik Pass. Inspection of individual cluster members shows that the wind at Senj is highly variable between different members and predominantly weak, so that a few relatively strong northeasterly bora cases dominate the average and result in the cluster centroid.

Independently of this analysis, Večenaj et al. (2011) discuss a possible lee rotor formation with reversed winds at Senj between 0000 and 1200 UTC 5 February 2005. The current analysis shows that this exact period belongs to cluster 7, and is immersed within a strong bora episode of cluster 2. The rotors over the eastern Adriatic have been reported in a number of studies (Belušić et al. 2007; Grubišić and Orlić 2007; Gohm et al. 2008; Prtenjak and Belušić 2009; Stiperski et al. 2012), but no systematic knowledge exists about their characteristics and locations. Presently, the only way to verify the hypothesis that a lee rotor formation is responsible for the flow behavior at Senj is to reproduce the situation with a numerical model. This is discussed in a later subsection.

b. Synoptic situation

Figure 7 depicts the mean surface synoptic situation obtained from the ERA-Interim reanalysis (Dee et al. 2011) for each cluster. Clusters 1 and 3 are both characterized by weak pressure gradients over the northeastern Adriatic, which favor the development of local mesoscale thermal circulations with low wind speeds, such as the sea/land breeze and katabatic/anabatic winds (e.g. Prtenjak et al. 2006; 2010). Weak synoptic-scale pressure gradient force from the southwest to northeast in cluster 1 might cause pressure-driven channeling (e.g. Carrera et al. 2009) through the Vratnik Pass and hence contribute to the southwesterly wind. However, cluster 1 most frequently occurs in the afternoon hours (not shown), indicating that a large percentage of its cases are related to mesoscale thermal circulations. MSLP for cluster 8 depicts the typical pattern related to the Adriatic sirocco, with the cyclone northwest of the region of interest (e.g. Jurčec et al. 1996; Pasarić et al. 2009).

The flow pattern in cluster 6 is most frequently a consequence of an early stage of the Genoa cyclone. It is more frequent in the afternoon hours than during the night (not shown). It thus appears that the alignment of the geostrophic wind with the afternoon thermal sea-breeze and anabatic circulations, together with the related channeling, results in strong southwesterly winds at the Vratnik Pass. The decoupling of winds at Rab from the southwesterly direction seen at all other stations in cluster 6 is evident also in the results of Pandžić and Likso (2005) for a similar wind pattern (their wind type 8). The exact reasons for this departure are not known, but it is probably related to the complexity of the coastal terrain (e.g. Nitis et al. 2005; Prtenjak et al. 2006). Inspection of the individual cluster members supports the latter: when the winds at Rab and Mali Lošinj are weak to moderate, which is most frequently the case in cluster 6, the wind pattern is very similar to the cluster centroid. However, when the surface wind speeds become higher, the wind direction at Rab aligns with the other stations and becomes southwesterly, implying that the synoptic flow overcomes the local effects.

Bora clusters (2, 4 and 5) are characterized by the typical northeasterly pressure gradient over the Dinaric Alps. The usual distinction between the cyclonic and anticyclonic bora (e.g. Jurčec 1981; Heimann 2001) is evident here too. Cluster 5 is the representative of the cyclonic bora, with the main generating factor being the Genoa cyclone that propagates along the Apennine peninsula towards the southeast. Cluster 2 represents the anticyclonic bora where the high-pressure center located northeast of the Adriatic ensures the supply of cold air impinging on the Dinaric Alps as the northeasterly wind. Cluster 4 is characterized by the weakest pressure gradients among the three bora clusters and individual charts show that it is predominantly the anticyclonic bora type, but that it can also be related to a cyclone (not shown).

The decoupled cases in the special bora cluster 7 are probably local phenomena, so synoptic charts do not provide much insight into their dynamics. The basic synoptic structure seems to be a mixture of an anticyclone affecting the northern Adriatic bora and a cyclone above the northeastern Mediterranean affecting the southern Adriatic bora.

c. Numerical simulations

The focus for numerical simulations is on the two puzzling clusters: cluster 7 for bora and cluster 8 for sirocco. Both were discussed above and here we report on the results of simulations of several cases from these two clusters. The Weather Research and Forecasting – Advanced Research WRF (WRF-ARW) model, version 3.3 (Skamarock et al. 2008) is used for this purpose. Initial and boundary conditions are obtained from the ERA-Interim reanalysis, available every 6 h. The setup consists of a number of nested domains with the outermost domain's grid spacing of 27 km being decreased by the factor of 3 for each nested domain. Two simulations are presented here: the grid spacing of the innermost domain is 1 km for the first and 1/3 km for the second simulation. Two-way nesting is used for the first and one-way for the second simulation. All domains are centered on the present region of interest (the locations of domains are shown in the figures below). There are 51 vertical levels, with the layer depths gradually increasing with height. Vertical mixing is parameterized using the Mellor-Yamada-Janjić scheme (Janjić 2002).

One of the questions raised above is about the origin of the unexpected northeasterly wind at the Vratnik Pass during the sirocco episodes of cluster 8. Figure 8 compares the measurements at the Vratnik Pass with the ERA-Interim reanalysis at the point closest to the Vratnik Pass for the long sirocco episode from 26 December – 28 December 2004. The ERA-Interim wind is persistently from the south until the end of the sirocco episode on 28 December 2004. Therefore, the common expectation for this case would be a persistent southwesterly wind at the Vratnik Pass, because one could assume that a synoptically southerly wind would be locally channeled through the gap as a southwesterly wind (e.g. Gaberšek and Durran 2006). However, the wind in the measurements is most frequently from the northeast with only shorter excursions to south and southwest. A similar disagreement between the measurements and reanalyses has been noticed for a number of other episodes as well. In order to study the cause of this discrepancy, a WRF simulation was run from 1200 UTC 26 December – 1200 UTC 28 December 2004. Figure 8 shows the comparison of wind directions between the WRF simulation and the measurements. Wind speeds are reproduced reasonably well by the model, but are not shown because they are not as relevant for this analysis. The two outer stations, Rab and Mali Lošinj, clearly indicate the existence of sirocco over the northern Adriatic and this is well reproduced by the model. The Vratnik Pass wind direction is simulated rather well after 00 UTC 27 December 2004. While the measured wind at Senj is predominantly from the southeast, the modeled direction at Senj is closely coupled with the modeled direction at the Vratnik Pass, particularly for larger changes of direction, and hence does not satisfactorily reproduce the local wind at Senj. This erroneous coupling between the Vratnik Pass and Senj winds is a common characteristic of many other model simulations performed for this study, regardless of the episode or the changes in the model setup. These unsuccessful simulations will not be reported here.

Since the modeled direction at the Vratnik Pass is satisfactory, we use the model for further analysis. Two different situations are compared. The surface fields from the ERA-Interim reanalysis and the WRF simulation at the two coarsest grids are shown in Fig. 9 at:

(i) 00 UTC 27 December, when ERA-Interim and WRF, and to a certain extent the measurements, agree that the wind at the Vratnik Pass is southerly, and

(ii) 06 UTC 27 December, when the measurements and WRF switch to northeasterly flow while ERA-Interim continues to experience the southerly flow.

The ERA-Interim spatial pattern does not change much between these two situations. The Genoa cyclone is shown to be the main generator of sirocco over the Adriatic and the southerly wind at the Vratnik Pass. The outermost WRF domain shows good broad agreement with the reanalysis for both situations. The major discrepancy is seen at 06 UTC, when a relatively small closed low-pressure center appears at the west Adriatic coast in the lee of the Apennines only in the

WRF simulation. The first nested domain with 9-km grid spacing provides more detailed view of the formation of the Adriatic low. It somewhat resembles the twin cyclone formation reported by Horvath et al. (2008), although here the Adriatic low is on a smaller spatial scale. This low bends the isobars over the northern Adriatic and as a result, the wind along the entire northeastern Adriatic turns to easterly and northeasterly direction while the wind further inland becomes easterly to southeasterly. It is this mesoscale wind pattern that forces the channeling of northeasterly wind through the Vratnik Pass. Further details of the flow channeling through the Vratnik Pass are seen from the two domains with smaller grid spacing, but they do not reveal relevant new information and are hence not shown. A similar synoptic situation, but with a more expressed Adriatic low, is seen in the hours following the observed southwesterly flow episode at the Vratnik Pass, thus after 20 UTC 27 December, and before the cessation of sirocco on 28 December. The quick formation and disappearance of the low at 00 UTC 27 December indicates that these secondary lows are transient features. The role of orography in their formation might be partially explained by the mechanisms suggested by Lin (2007), but the detailed analysis of these processes is beyond the scope of this study.

Another simulation was performed for the cluster-7 episode of 5 February 2005, in order to examine a possible rotor occurrence at Senj (Večenaj et al. 2011) as one of the mechanisms leading to the directional decoupling between the Vratnik Pass and Senj. Figure 10 shows that the model correctly captures the onset and the first few hours of flow reversal at Senj, and that the reversal lasts longer for the domain with smaller grid spacing. It should be mentioned that this simulation is the only one that successfully reproduced the Vratnik Pass–Senj decoupling, and this was achieved only after changing the nesting procedure from two-way to one-way. This indicates the high sensitivity of these flow features to details of the model setup, which is in accordance with the conclusions of Gohm et al. (2008). Figure 11 depicts an example of the flow structure during the flow reversal for the innermost domain. There are several disconnected regions of reversed flow just downstream of the mountains that sometimes cover the coastal areas and extend over the sea. These features are highly variable in appearance, extent and duration. The vertical cross-section indicates the existence of a rotor circulation above Senj. The rotor occurs under an undular bore located downstream and below a wave-breaking region, which agrees well with previous studies on rotor dynamics (e.g. Jiang et al. 2007; Smith and Skyllingstad 2009; Stiperski et al. 2012). These results confirm that some of the decoupled situations arise from local rotor circulations. A detailed analysis of this case is left for a separate study.

5. Conclusions

First wind measurements over an extended time period at the Vratnik Pass, a mountain gap in the Dinaric Alps, were performed from October 2004 – June 2005. Wind roses and cluster analysis reveal that the winds through the Vratnik Pass are highly polarized and come from the two main directions that are parallel to the axis of the gap. These flow patterns depend on the synoptic-scale forcing, but the resulting gap flow is governed by the mesoscale pressure gradient, in accordance with the results of Gaberšek and Durran (2006).

Quite expectedly, moderate to strong northeasterly wind is more frequent and is usually, but not always, related to the northeasterly bora wind at the downstream town of Senj. An unforeseen result is a large number of cases with northeasterly winds at the Vratnik Pass that are decoupled from the winds at Senj. While some of these cases are related to low wind speeds or a shallow southeasterly Adriatic sirocco flow, there are a considerable number of other cases that could not be explained easily. Even the clustering method has grouped the latter cases into a separate cluster. The WRF-ARW model was able to reproduce only one case of the directional decoupling, which was related to a mountain-lee rotor.

Another unexpected result that disagrees with the previous limited knowledge is the predominance of northeasterly wind at the Vratnik Pass during the Adriatic sirocco episodes. Using a successful WRF-ARW simulation of one such episode, this discrepancy is shown to be a consequence of a mesoscale low-pressure center developing over the Adriatic and is apparently unrelated to the local terrain surrounding the Vratnik Pass.

Southwesterly wind at the Vratnik Pass is less frequent and is largely related to situations with very weak synoptic pressure gradient when weak mesoscale see-breeze and anabatic circulations dominate (e.g. Prtenjak 2003). Stronger southwesterly wind at the Vratnik Pass appears when this weak circulation is superimposed on a geostrophic wind in the same direction. An additional mechanism for the latter could be the generation of a large mountain wave with a strong southeasterly wind in the lee. These flow conditions have not been studied previously, so further analysis is needed for understanding of the exact mechanisms.

Several interesting dynamical and modeling problems emerge from this study. The model difficulty to reproduce the directional bora decoupling between the Vratnik Pass and Senj is an important challenge for the modeling community. Simulations with different model setups indicate that the model is able to reproduce the decoupling only for a specific constellation of input parameters, which in one case amounted to using one-way instead of two-way nesting. The decoupling is also an interesting dynamical issue, since lee rotors have been reported in many occasions over the Adriatic, but their frequencies, locations and mechanisms are generally not known. The appearance of a relatively small-scale closed low-pressure center over the Adriatic in the lee of the Apennines that is associated with the Genoa cyclone calls for further analysis in order to understand the mechanisms that generate such systems. It is not known how many cases from cluster 8 are related to those systems, but the predominance of northeasterly winds at the Vratnik Pass in cluster 8 indicates that these might be more than rare events. Two features worthy of further investigation emerge also in cluster 6: strong southwesterly winds at the Vratnik Pass in otherwise weak-wind flow that could be related to mountain-wave dynamics, and the strange 90° departure of wind direction at Rab that was only hypothetically related to the influence of the local terrain.

Acknowledgments

We thank Vlatko Vukičević for useful discussions about the Adriatic sirocco wind and Maja Telišman Prtenjak for providing the information about the wind sheltering at the measurement stations Rab and Mali Lošinj. Three anonymous reviewers are gratefully acknowledged for their constructive comments and suggestions. The Croatian Meteorological and Hydrological Service kindly provided the data at Rab and Mali Lošinj. The work was partially supported by the Croatian Ministry of Science, Education and Sports (projects BORA 119-1193086-1311 and AQCT 119-1193086-1323) and the Croatian Science Foundation (project CATURBO 09/151).

References

Anderberg, M. R., 1973: *Cluster Analysis for Applications*. Academic Press, 359 pp.

Belušić, D., and I. Güttler, 2010: Can mesoscale models reproduce meandering motions? *Q. J. Roy. Meteor. Soc.*, **136**, 553–565.

Belušić, D., and Z. B. Klaić, 2006: Mesoscale dynamics, structure and predictability of a severe Adriatic bora case. *Meteor. Z.*, **15**, 157–168.

Belušić, D., M. Žagar, and B. Grisogono, 2007: Numerical simulation of pulsations in the bora wind. *Q. J. Roy. Meteor. Soc.*, **133**, 1371–1388.

Brzović, N., and N. Strelec Mahović, 1999: Cyclonic activity and severe jugo in the Adriatic. *Phys. Chem. Earth*, **24**, 653–657.

Burlando, M., M. Antonelli, and C. F. Ratto, 2008: Mesoscale wind climate analysis: identification of anemological regions and wind regimes. *Int. J. Climatol.*, **28**: 629–641.

Carrera, M. L., J. R. Gyakum, and C. A. Lin, 2009: Observational study of wind channeling within the St. Lawrence River Valley. *J. Appl. Meteor. Climatol.*, **48**, 2341–2361.

Dee, D. P., S. M. Uppala, A. J. Simmons, P. Berrisford, P. Poli, S. Kobayashi, U. Andrae, M. A. Balmaseda, G. Balsamo, P. Bauer, P. Bechtold, A. C. M. Beljaars, L. van de Berg, J. Bidlot, N. Bormann, C. Delsol, R. Dragani, M. Fuentes, A. J. Geer, L. Haimberger, S. B. Healy, H. Hersbach, E. V. Hólm, L. Isaksen, P. Kållberg, M. Köhler, M. Matricardi, A. P. McNally, B. M. Monge-Sanz, J.-J. Morcrette, B.-K. Park, C. Peubey, P. de Rosnay, C. Tavolato, J.-N. Thépaut, and F. Vitart, 2011: The ERA-Interim reanalysis: configuration and performance of the data assimilation system. *Q. J. Roy. Meteor. Soc.*, **137**, 553–597.

Dorman, C. E., S. Carniel, L. Cavaleri, M. Sclavo, J. Chiggiato, J. Doyle, T. Haack, J. Pullen, B. Grbec, I. Vilibić, I. Janeković, C. Lee, V. Malačić, M. Orlić, E. Paschini, A. Russo, and R. P. Signell, 2006: February 2003 marine atmospheric conditions and the bora over the northern Adriatic, *J. Geophys. Res.*, **111**, C03S03, doi:10.1029/2005JC003134 [printed 11 2 (C3), 2007].

Elsner, J. B., 2003: Tracking hurricanes. *Bull. Amer. Meteor. Soc.*, **84**, 353–356.

Gaberšek, S., and D. R. Durran, 2006: Gap flows through idealized topography. Part II: Effects of rotation and surface friction. *J. Atmos. Sci.*, **63**, 2720–2739.

Gohm, A. and G. J. Mayr, 2005: Numerical and observational case-study of a deep Adriatic bora. *Q. J. Roy. Meteor. Soc.*, **131**, 1363–1392.

Gohm, A., G. J. Mayr, A. Fix, and A. Giez, 2008: On the onset of bora and the formation of rotors and jumps near a mountain gap. *Q. J. Roy. Meteor. Soc.*, **134**, 21–46.

Grisogono, B., and D. Belušić, 2009: A review of recent advances in understanding the meso- and microscale properties of the severe Bora wind. *Tellus*, **61A**, 1–16.

Grubišić, V., 2004: Bora-driven potential vorticity banners over the Adriatic. *Q. J. Roy. Meteor. Soc.*, **130**, 2571–2603.

Grubišić V., and M. Orlić, 2007: Early observations of rotor clouds by Andrija Mohorovičić. *Bull. Amer. Meteor. Soc.*, **88**, 693–700.

Heimann, D., 2001: A model-based wind climatology of the eastern Adriatic coast. *Meteor. Z.*, **10**, 5–16.

Horvath, K., Y.-L. Lin, and B. Ivančan-Picek, 2008: Classification of cyclone tracks over the Apennines and the Adriatic Sea. *Mon. Wea. Rev.*, **136**, 2210–2227.

Ivančan-Picek, B., V. Jurčec and D. Drvar, 2006: On the causes of Adriatic Jugo wind variations. *Cro. Meteor. J.*, **41**, 21–32.

Janjić, Z. I., 2002: Nonsingular implementation of the Mellor–Yamada level 2.5 scheme in the NCEP meso model. *NCEP Office Note*, No. 437, 61 pp.

Jiang, Q. F., and J. D. Doyle, 2005: Wave breaking induced surface wakes and jets observed during a Bora event. *Geophys. Res. Let.,* **32**, L17807, doi:10.1029/2005GL022398.

Jiang, Q., J. D. Doyle, S. Wang, and R. B. Smith, 2007: On boundary layer separation in the lee of mesoscale topography. *J. Atmos. Sci.*, **64**, 401–420.

Jiménez, P. A., J. F. González-Rouco, J. P. Montávez, E. García-Bustamante, and J. Navarro, 2009: Climatology of wind patterns in the northeast of the Iberian Peninsula. *Int. J. Climatol.*, **29**, 501–525.

Jurčec, V., 1981: On mesoscale characteristics of Bora conditions in Yugoslavia. *Pure Appl. Geophys.*, **119**, 640–657.

Jurčec, V., B. Ivančan-Picek, V. Tutiš, and V. Vukičević, 1996: Severe Adriatic jugo wind. *Meteor. Z.*, **N.F. 5**, 67–75.

Kaufmann, P., and R. O. Weber, 1996: Classification of mesoscale wind fields in the MISTRAL field experiment. *J. Appl. Meteor.*, **35**, 1963–1979.

Kaufmann, P., and C. D. Whiteman, 1999: Cluster-analysis classification of wintertime wind patterns in the grand canyon region. *J. Appl. Meteor.*, **38**, 1131–1147.

Klaić, Z. B., Z. Pasarić, and M. Tudor, 2009a: On the interplay between sea-land breezes and Etesian winds over the Adriatic, *J. Mar. Syst.*, **78**, S101–S118.

Klaić, Z. B., A. D. Prodanov, and D. Belušić, 2009b: Wind measurements in Senj - underestimation of true bora flows. *Geofizika*, **26**, 245–252.

Klemp, J. B. and D. R. Durran, 1987: Numerical modelling of bora winds. *Meteorol. Atmos. Phys.*, **36**, 215–227.

Lin, Y.-L., 2007: *Mesoscale dynamics*. Cambridge University Press, 630 pp.

Mahrt, L., 2010: Common microfronts and other solitary events in the nocturnal boundary layer. *Q. J. Roy. Meteor. Soc.*, **136**, 1712–1722.

Mahrt, L., 2011: Surface wind direction variability. *J. Appl. Meteor. Climatol.*, **50**, 144–152.

Makjanić, B., 1978: Bura, jugo, etezija, Prilozi poznavanju vremena i klime SFRJ. Savezni meteorološki zavod, (in Croatian).

Nitis, T., D. Kitsiou, Z. B. Klaić, M. T. Prtenjak, and N. Moussiopoulos, 2005: The effects of basic flow and topography on the development of the sea breeze over a complex coastal environment. *Q. J. Roy. Meteor. Soc.*, **131**, 305–328.

Orlić, M., B. Penzar, and I. Penzar, 1988: Adriatic sea and land breezes: clockwise versus anticlockwise rotation. *J. Appl. Meteor.*, **27**, 675–679.

Pandžić, K., and T. Likso, 2005: Eastern Adriatic typical wind field patterns and large-scale atmospheric conditions. *Int. J. Climatol.*, **25**, 81–98.

Pasarić, Z., D. Belušić, and Z. B. Klaić, 2007: Orographic influences on the Adriatic sirocco wind. *Ann. Geophys.*, **25**, 1263–1267.

Pasarić, Z., D. Belušić, and J. Chiggiato, 2009: Orographic effects on meteorological fields over the Adriatic from different models. *J. Mar. Syst.*, **78**, S90–S100.

Poje, D., 1992: Wind persistence in Croatia. *Int. J. Climatol.*, **12**, 569–586.

Pope, M., C. Jakob, and M. Reeder, 2009: Objective classification of tropical mesoscale convective systems. *J. Climate*, **22**, 5797–5808.

Prtenjak, M. T., 2003: Main characteristics of sea/land breezes along the eastern coast of the Northern Adriatic. *Geofizika*, **20**, 75–92

Prtenjak, M. T., B. Grisogono, and T. Nitis, 2006: Shallow mesoscale flows at the north-eastern Adriatic coast. *Q. J. Roy. Meteor. Soc.*, **132**, 2191–2216.

Prtenjak, M. T., and B. Grisogono, 2007: Sea-land breeze climatological characteristics along the northern Croatian Adriatic coast. *Theor. Appl. Climatol.*, **90**, 201–215.

Prtenjak, M. T., Z. Pasarić, M. Orlić, and B. Grisogono, 2008: Rotation of sea-land breezes along the northeastern Adriatic coast. *Ann. Geophys.*, **26**, 1711–1724.

Prtenjak, M. T., and D. Belušić, 2009: Formation of reversed lee flow over the north-eastern Adriatic during bora. *Geofizika*, **26**, 145–155.

Prtenjak, M. T., M. Viher, and J. Jurković, 2010: Sea-land breeze development during a summer bora event along the north-eastern Adriatic coast. *Q. J. Roy. Meteor. Soc.*, **136**, 1554–1571.

Signell, R. P., J. Chiggiato, J. Horstmann, J. D. Doyle, J. Pullen, and F. Askari, 2010: High ‐ resolution mapping of Bora winds in the northern Adriatic Sea using synthetic aperture radar. *J. Geophys. Res.*, **115**, C04020, doi:10.1029/2009JC005524.

Skamarock, W. C., J. B. Klemp, J. Dudhia, D. O. Gill, D. M. Barker, M. G. Duda, X.-Y. Huang, W. Wang, and J. G. Powers, 2008: A description of the Advanced Research WRF Version 3. NCAR/TN–475+STR.

Smith, R. B., 1987: Aerial observations of the Yugoslavian bora. *J. Atmos. Sci.,* **44**, 269–297.

Smith, C. M., and E. D. Skyllingstad, 2009: Investigation of upstream boundary layer influence on mountain wave breaking and lee wave rotors using a large-eddy simulation. *J. Atmos. Sci.*, **66**, 3147–3164.

Stiperski, I., B. Ivančan-Picek, V. Grubišić, and A. Bajić, 2012: Complex bora flow in the lee of Southern Velebit. *Q. J. Roy. Meteor. Soc.*, **138**, 1490–1506.

Večenaj, Ž., D. Belušić, and B. Grisogono, 2010: Characteristics of the near-surface turbulence during a bora event. *Ann. Geophys.*, **28**, 155–163.

Večenaj, Ž., D. Belušić, and B. Grisogono, 2011: A case study of severe bora event at Vratnik Pass and Senj, NE Adriatic coast. *31st International Conference on Alpine Meteorology*, Aviemore, UK, 23 – 27 May 2011.

Večenaj, Ž., D. Belušić, V. Grubišić, and B. Grisogono, 2012: Along-coast features of bora-related turbulence. *Boundary-Layer Meteor.*, **143**, 527–545.

Vukičević, V., V. Jurčec, and B. Ivančan-Picek, 2005: Adriatic jugo wind during 2000 – 2004. *Cro. Meteor. J.*, **40**, 418–421.

Weber, R. O., and P. Kaufmann, 1995: Automated classification scheme for wind fields. *J. Appl. Meteor.*, **78**, 1133–1141.

Yoshino, M. M., 1976: *Local wind bora*. University of Tokyo Press, 289 pp.

TABLES

Table 1. A contingency table for the simultaneous occurrence of Bora at the Vratnik Pass (VP) and Senj. Each event at each site has a numerical value assigned to it (in brackets). Different combinations of events observed simultaneously at both sites result in different detector values in the table (see Fig. 4). NaN denotes a data gap.

Senj / VP	Bora YES (1)	Bora NO (0)	NaN (-0.25)
Bora YES (2)	3	2	1.75
Bora NO (0)	1	0	-0.25
NaN (-0.75)	0.25	-0.75	-1

Table 2. Number (N) and percentage of cases, and the average episode duration (T) for each cluster. Trans denotes other cluster categories that each cluster most frequently transitions to.

Cluster	1	2	3	4	5	6	7	8
N	810	711	689	615	278	273	224	130
[%]	21.7	19.1	18.5	16.5	7.5	7.3	6.0	3.5
T (h)	8.4	8.3	5.2	5.2	9.6	10.5	5.2	5.7
Trans	3, 6	4, 5	1, 4	2, 3, 7	2	1	4, 3, 2	3, 1

FIGURE CAPTIONS

Figure 1. Topography of the northeastern Adriatic region. The four observational stations are indicated: Vratnik Pass (44.979°N, 14.984°E, 698 m above MSL), Senj (44.990°N, 14.899°E, 2 m above MSL), Rab (44.750°N, 14.767°E, 24 m above MSL), and Mali Lošinj (44.533°N, 14.467°E, 53 m above MSL). The inset in the upper right corner shows the detailed topography around the Vratnik Pass (contour interval is 75 m).

Figure 2. Wind roses at (a) the Vratnik Pass, (b) Senj, (c) Rab and (d) Mali Lošinj for the period from October 2004 to June 2005.

Figure 3. Conditional wind roses at Senj during October 2004 – June 2005 for six different wind speed and direction combinations at the Vratnik Pass. Headers at each subplot denote criteria at the Vratnik Pass for which conditional wind rose at Senj was calculated: (a), (b) and (c) for northeasterly bora direction; (d), (e) and (f) for southwesterly direction; (a) and (d) for weak winds, (b) and (e) for moderate winds, (c) and (f) for strong winds at the Vratnik Pass. The remaining cases (2%) are predominantly related to weak winds at the Vratnik Pass from directions other than bora and southwesterly.

Figure 4. Detection of the simultaneous bora occurrence at the Vratnik Pass and Senj. The detector value of 2 denotes the decoupled episodes that occur when bora blows at the Vratnik Pass but not at Senj. The values 3 and 0 stand for the

bora presence and absence at both stations, respectively. See Table 1 for the complete description of the detector values.

Figure 5. Eight wind regimes represented by the K-means cluster centers. N denotes the number of members in a cluster. Bottom left in each panel is the 5 m s^{-1} reference vector.

Figure 6. Relative frequency distribution of the decoupled bora cases over different clusters. The numbers above bars denote the relative contribution of the decoupled cases to each cluster, expressed as the percentage of the total number of cases in a cluster. Zeros for clusters 1, 5 and 6 indicate that there are no decoupled bora episodes associated with these clusters.

Figure 7. MSLP for each cluster (see Fig. 5), averaged over all members of a cluster. The filled circle denotes the Vratnik Pass.

Figure 8. Surface wind direction at the four studied stations from measurements and the second nested WRF domain with 3-km grid spacing. ERA-Interim, available every 6 h, is additionally shown at the point closest to the Vratnik Pass.

Figure 9. MSLP and surface wind vectors from the ERA-Interim reanalysis and WRF outermost and first nested domains on 27 December 2004 at 00 UTC (left) and 06 UTC (right). Bottom left in each panel is the 20 m s^{-1} reference vector and the circle denotes the Vratnik Pass.

Figure 10. Modeled vs. measured wind speed (top panels) and direction (bottom panels) at the Vratnik Pass (left panels) and Senj (right panels) for the directionally decoupled bora episode from cluster 7 that occurred from 00 – 12 UTC 5 February 2005. Model results are shown for two domains with grid spacing of 1 km and 1/3 km.

Figure 11. The rotor occurrence in the WRF simulation of the decoupled bora episode at 03 UTC 5 February 2005 for the 1/3 km domain. (a) Wind vectors and the zonal wind component (color) at the first model level are shown over a subset of the domain. Axes labels are grid points. Regions of flow reversal are colored blue. Black circles denote Senj and the Vratnik Pass, and the black line indicates the location of the vertical cross-section. (b) The vertical cross-section along the indicated line, showing the wind vectors, turbulent kinetic energy (color) and isentropes (0.5 K interval).

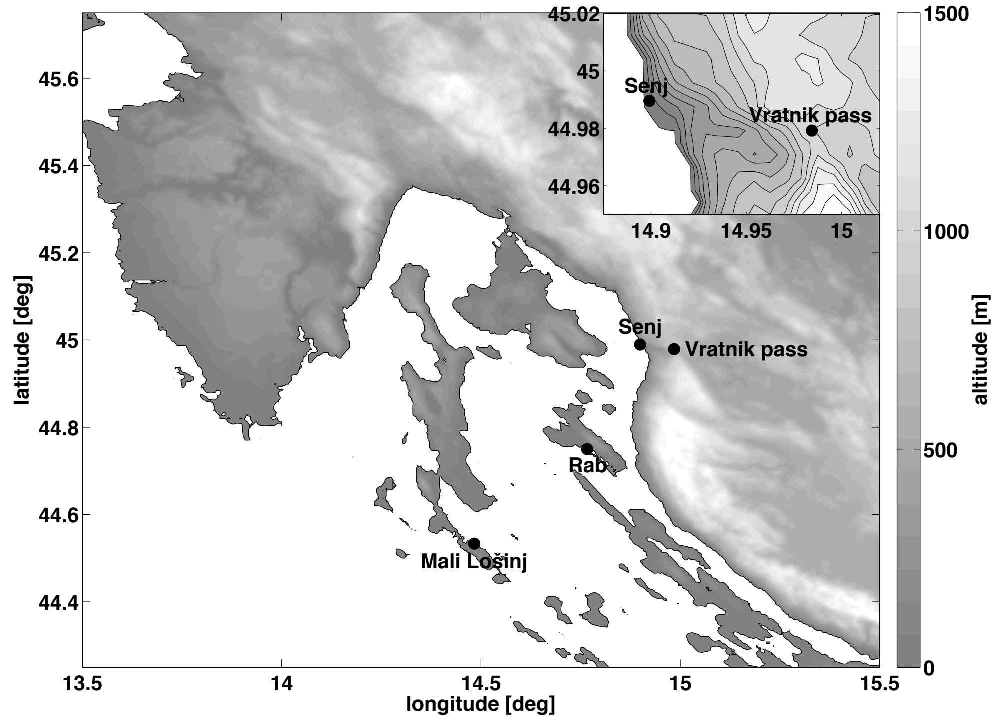

Figure 1. Topography of the northeastern Adriatic region. The four observational stations are indicated: Vratnik Pass (44.979°N, 14.984°E, 698 m above MSL), Senj (44.990°N, 14.899°E, 2 m above MSL), Rab (44.750°N, 14.767°E, 24 m above MSL), and Mali Lošinj (44.533°N, 14.467°E, 53 m above MSL). The inset in the upper right corner shows the detailed topography around the Vratnik Pass (contour interval is 75 m).

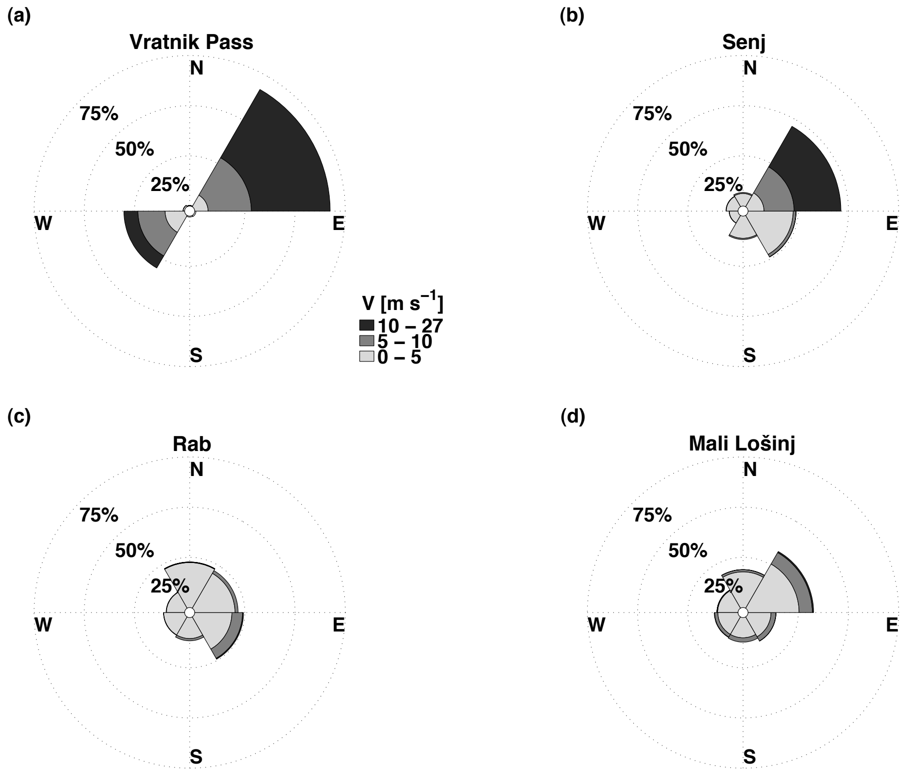

Figure 2. Wind roses at (a) the Vratnik Pass, (b) Senj, (c) Rab and (d) Mali Lošinj for the period from October 2004 to June 2005.

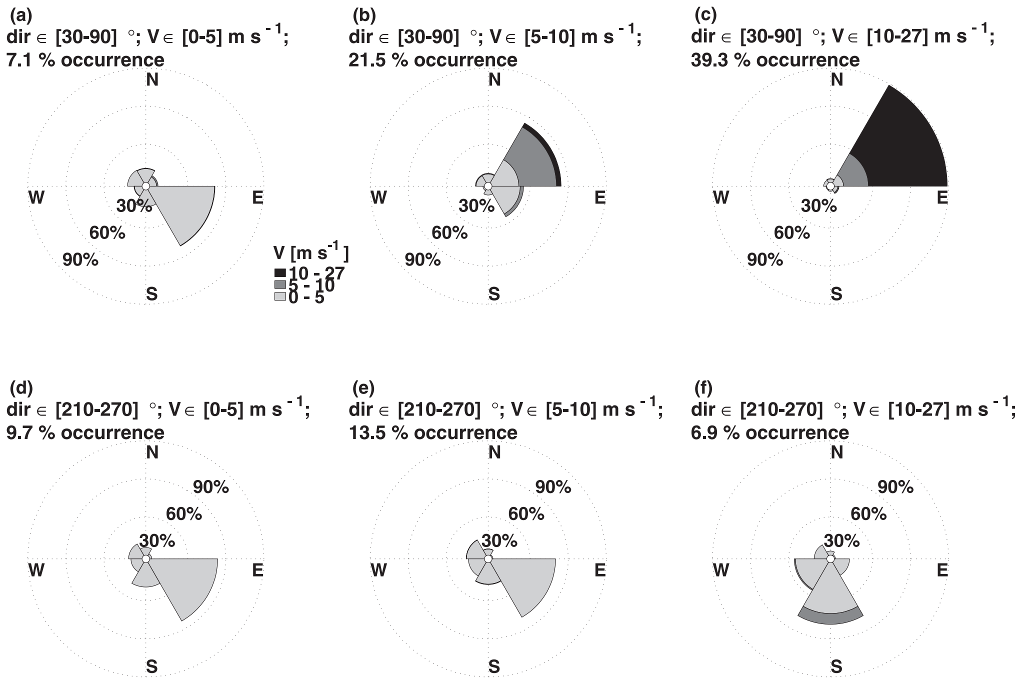

Figure 3. Conditional wind roses at Senj during October 2004 – June 2005 for six different wind speed and direction combinations at the Vratnik Pass. Headers at each subplot denote criteria at the Vratnik Pass for which conditional wind rose at Senj was calculated: (a), (b) and (c) for northeasterly bora direction; (d), (e) and (f) for southwesterly direction; (a) and (d) for weak winds, (b) and (e) for moderate winds, (c) and (f) for strong winds at the Vratnik Pass. The remaining cases (2%) are predominantly related to weak winds at the Vratnik Pass from directions other than bora and southwesterly.

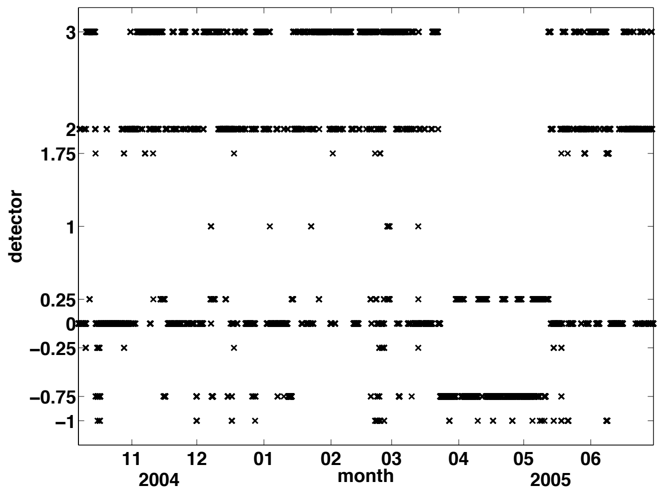

Figure 4. Detection of the simultaneous bora occurrence at the Vratnik Pass and Senj. The detector value of 2 denotes the decoupled episodes that occur when bora blows at the Vratnik Pass but not at Senj. The values 3 and 0 stand for the bora presence and absence at both stations, respectively. See Table 1 for the complete description of the detector values.

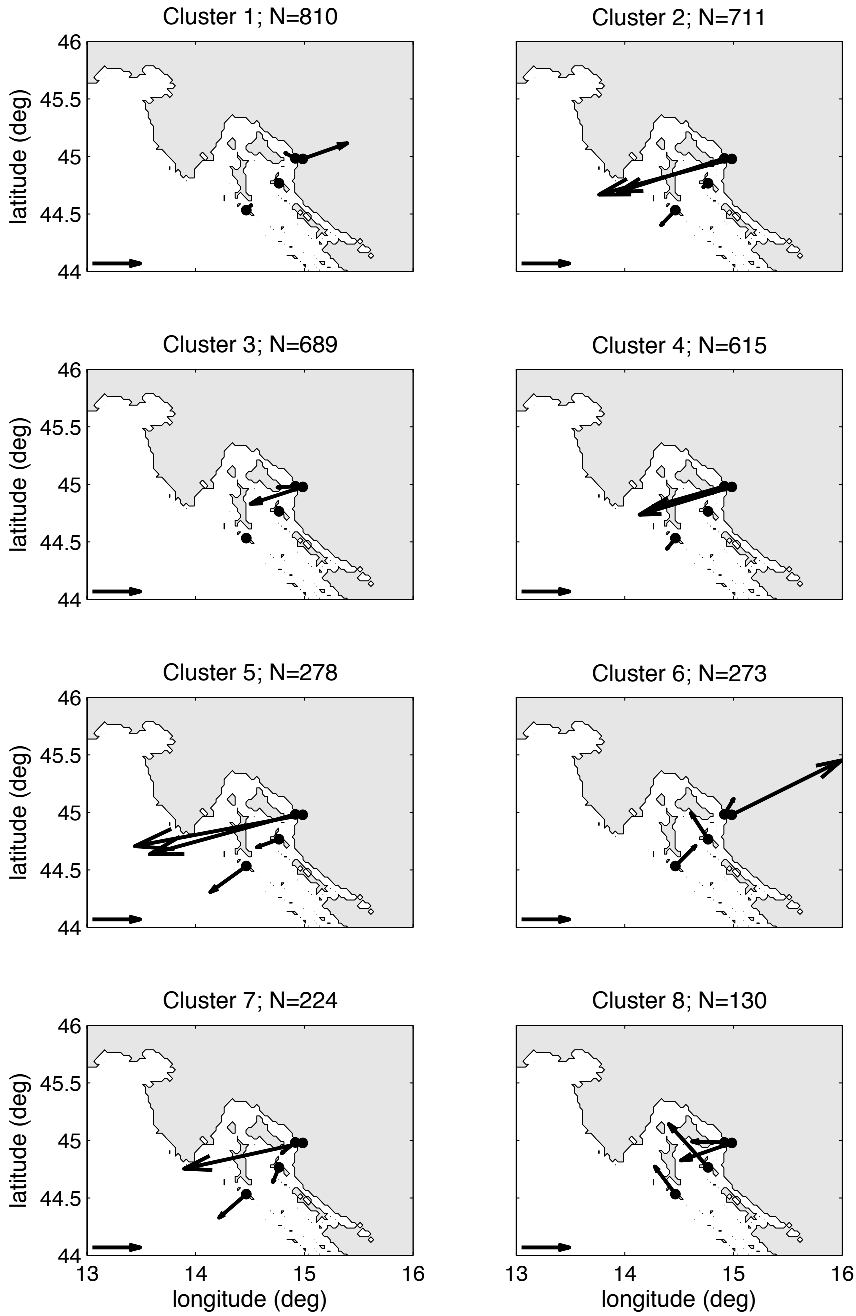

Figure 5. Eight wind regimes represented by the K-means cluster centers. N denotes the number of members in a cluster. Bottom left in each panel is the 5 m s^{-1} reference vector.

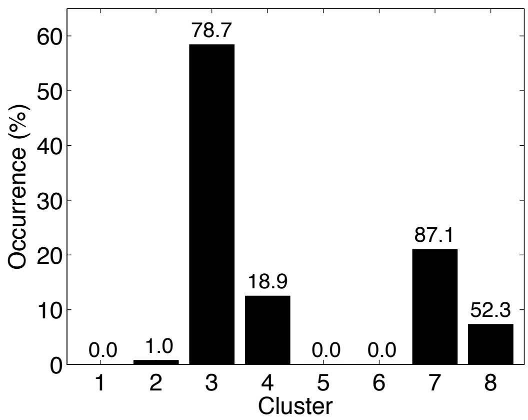

Figure 6. Relative frequency distribution of the decoupled bora cases over different clusters. The numbers above bars denote the relative contribution of the decoupled cases to each cluster, expressed as the percentage of the total number of cases in a cluster. Zeros for clusters 1, 5 and 6 indicate that there are no decoupled bora episodes associated with these clusters.

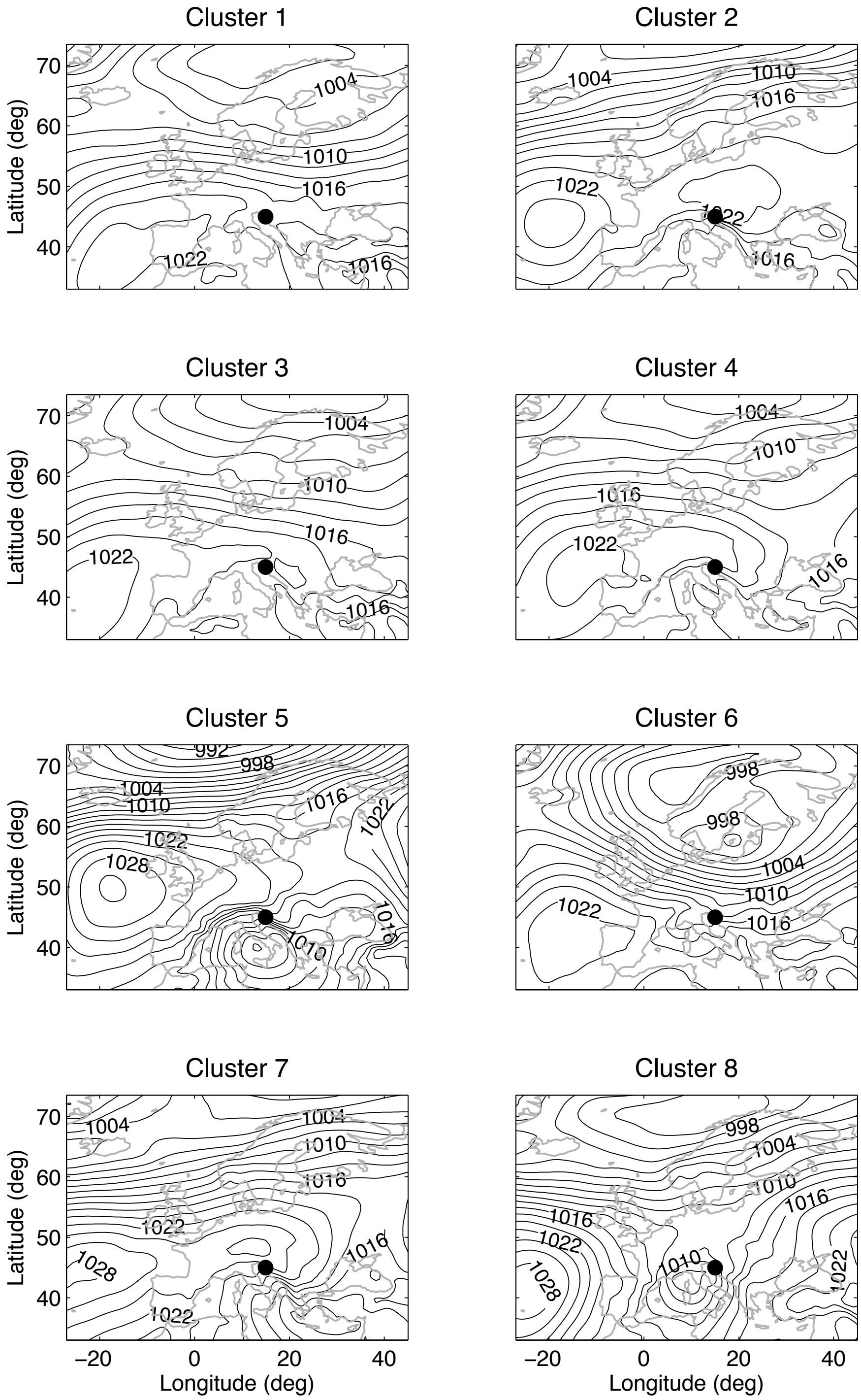

Figure 7. MSLP for each cluster (see Fig. 5), averaged over all members of a cluster. The filled circle denotes the Vratnik Pass.

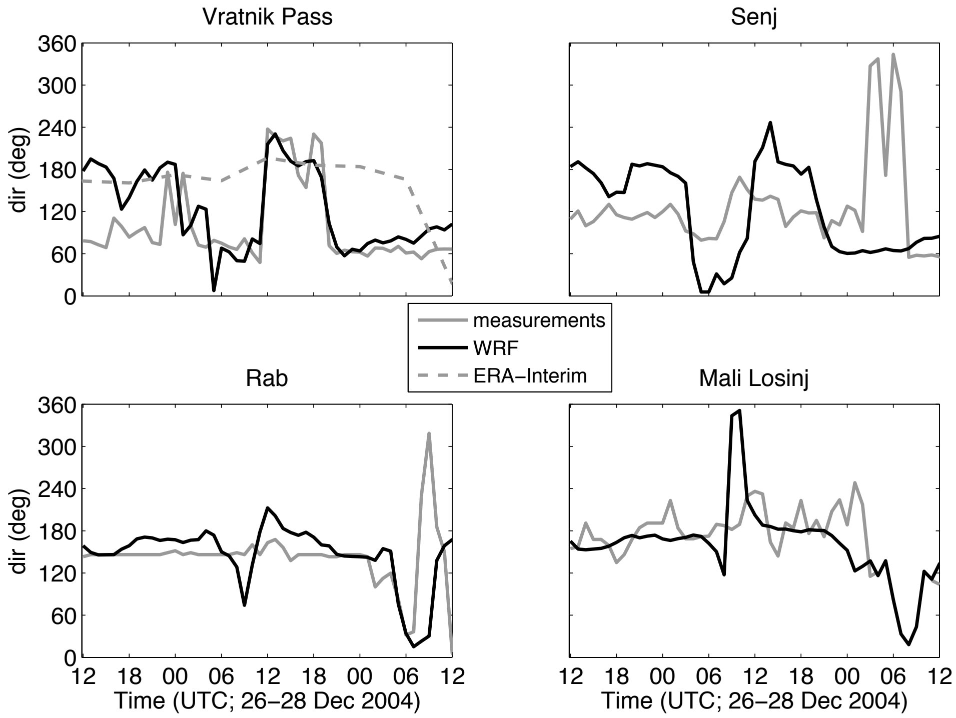

Figure 8. Surface wind direction at the four studied stations from measurements and the second nested WRF domain with 3-km grid spacing. ERA-Interim, available every 6 h, is additionally shown at the point closest to the Vratnik Pass.

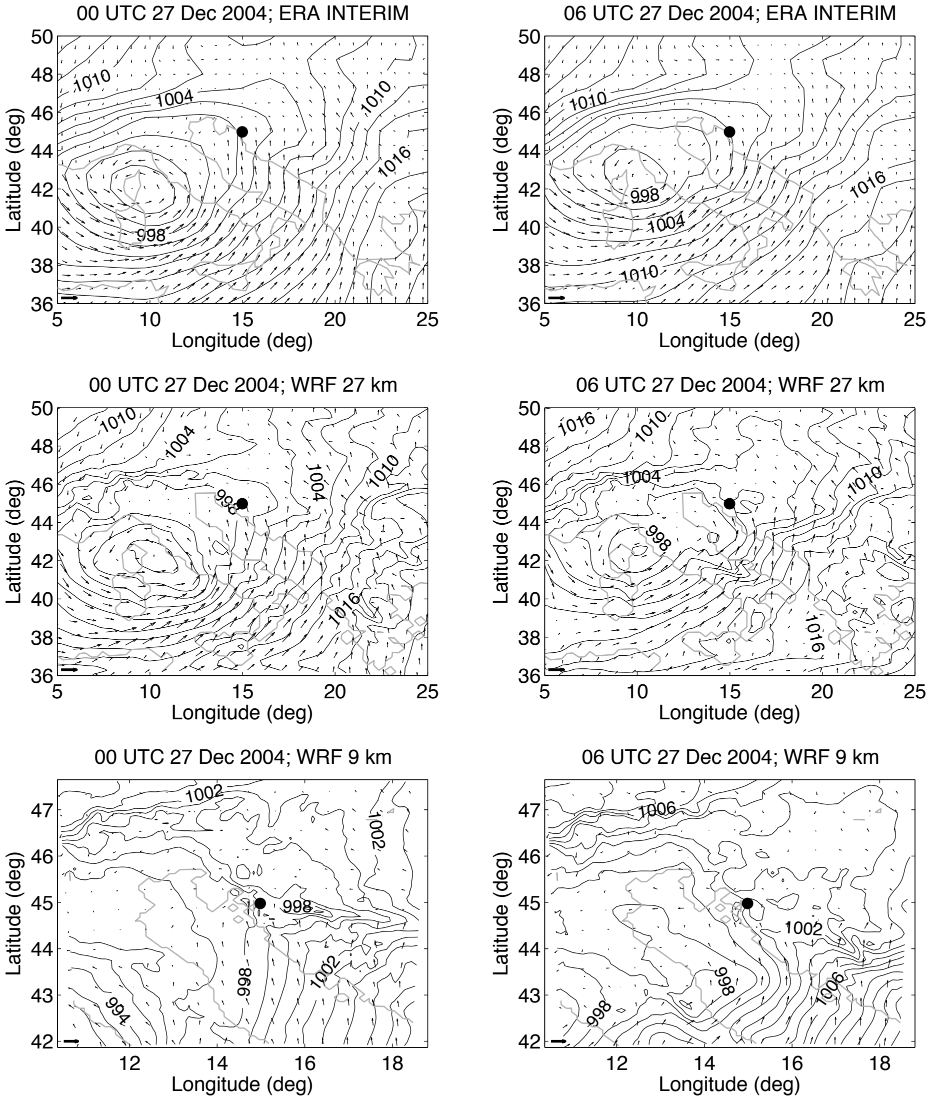

Figure 9. MSLP and surface wind vectors from the ERA-Interim reanalysis and WRF outermost and first nested domains on 27 December 2004 at 00 UTC (left) and 06 UTC (right). Bottom left in each panel is the 20 m s^{-1} reference vector and the filled circle denotes the Vratnik Pass.

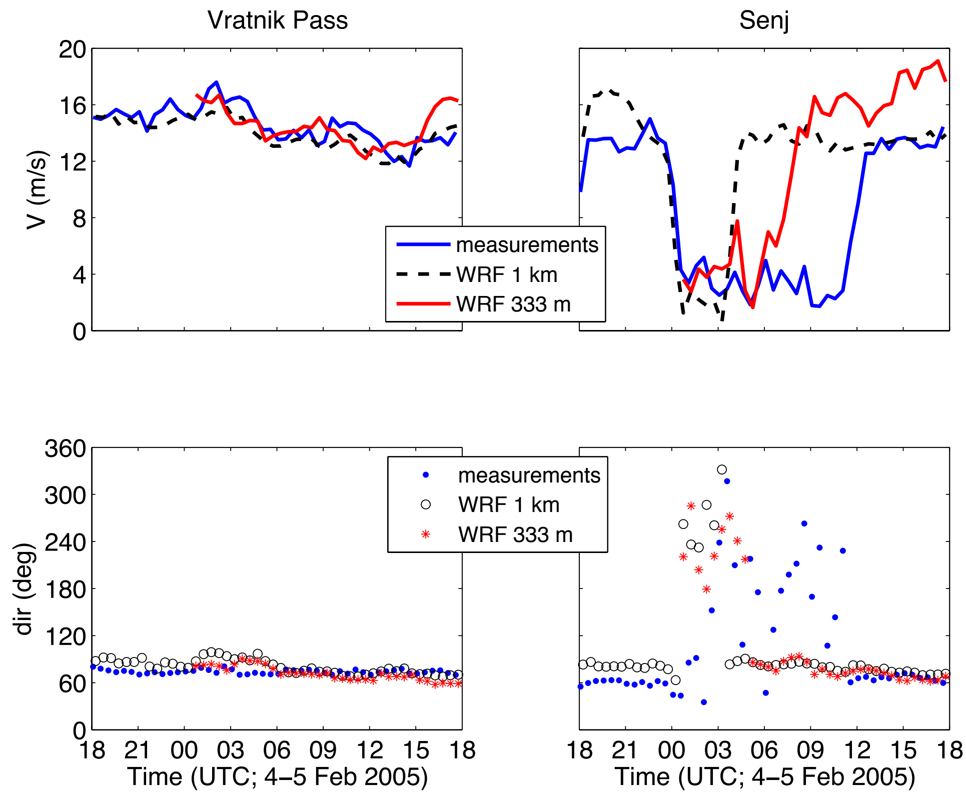

Figure 10. Modeled vs. measured wind speed (top panels) and direction (bottom panels) at the Vratnik Pass (left panels) and Senj (right panels) for the directionally decoupled bora episode from cluster 7 that occurred from 00 – 12 UTC 5 February 2005. Model results are shown for two domains with grid spacing of 1 km and 1/3 km.

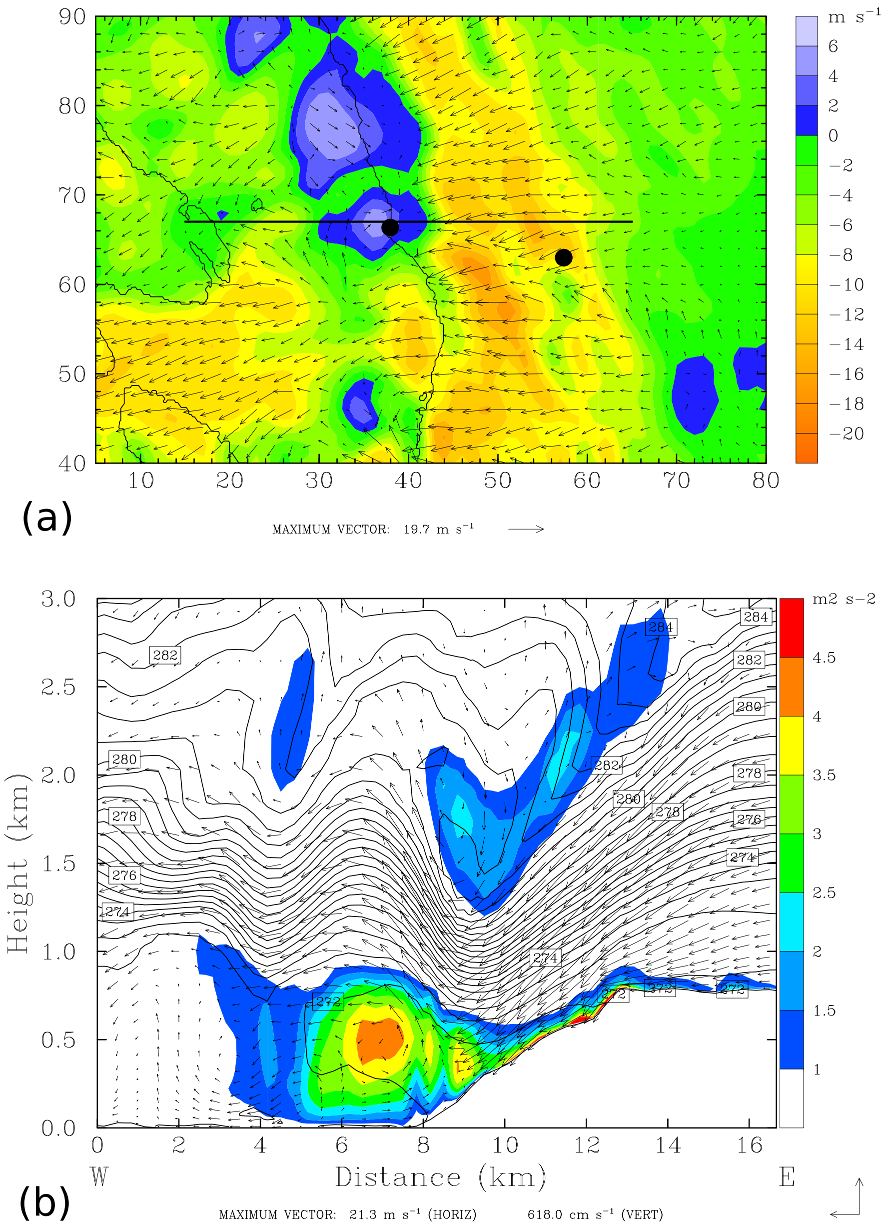

Figure 11. The rotor occurrence in the WRF simulation of the decoupled bora episode at 03 UTC 5 February 2005 for the 1/3 km domain. (a) Wind vectors and the zonal wind component (color) at the first model level are shown over a subset of the domain. Axes labels are grid points. Regions of flow reversal are colored blue. Black filled circles denote Senj and the Vratnik Pass, and the black line indicates the location of the vertical cross-section. (b) The vertical cross-section along the indicated line, showing the wind vectors, turbulent kinetic energy (color) and isentropes (0.5 K interval).